Molecular Pathways Differentiate Hepatitis C Virus (HCV) Recurrence from Acute Cellular Rejection in HCV Liver Recipients

Ricardo Gehrau,[1] Daniel Maluf,[1] Kellie Archer,[2] Richard Stravitz,[1] Jihee Suh,[1] Ngoc Le,[1] and Valeria Mas[1,3]

[1]Department of Surgery, [2]Biostatistics, and [3]Pathology, Virginia Commonwealth University, Richmond, Virginia, United States of America

Acute cellular rejection (ACR) and hepatitis C virus (HCV) recurrence (HCVrec) are common complications after liver transplantation (LT) in HCV patients, who share common clinical and histological features, making a differential diagnosis difficult. Fifty-three liver allograft samples from unique HCV LT recipients were studied using microarrays, including a training set (n = 32) and a validation set (n = 19). Two no-HCV-ACR samples from LT recipients were also included. Probe set intensity values were obtained using the robust multiarray average method (RMA) method. Analysis of variance identified statistically differentially expressed genes ($P \leq 0.005$). The *limma* package was used to fit the mixed-effects models using a restricted maximum likelihood procedure. The last absolute shrinkage and selection operator (LASSO) model was fit with HCVrec versus ACR as the dependent variable predicted. *N*-fold cross-validation was performed to provide an unbiased estimate of generalization error. A total of 179 probe sets were differentially expressed among groups, with 71 exclusive genes between HCVrec and HCV-ACR. No differences were found within ACR group (HCV-ACR vs. no-HCV-ACR). Supervised clustering analysis displayed two clearly independent groups, and no-HCV-ACR clustered within HCV-ACR. HCVrec-related genes were associated with a cytotoxic T-cell profile, and HCV-ACR–related genes were associated with the inflammatory response. The best-fitting LASSO model classifier accuracy, including 15 genes, has an accuracy of 100% in the training set. *N*-fold cross-validation accuracy was 78.1%, and sensitivity, specificity and positive and negative predictive values were 50.0%, 90.9%, 71.4% and 80.0%, respectively. *Arginase type II* (*ARG2*), *ethylmalonic encephalopathy 1* (*ETHE1*), *transmembrane protein 176A* (*TMEM176A*) and *TMEM176B* genes were significantly confirmed in the validation set. A molecular signature capable of distinguishing HCVrec and ACR in HCV LT recipients was identified and validated.

INTRODUCTION

Liver transplantation (LT) is the chosen treatment for patients with advanced liver disease and cirrhosis (http://optn.transplant.hrsa.gov). End-stage liver disease associated with hepatitis C virus (HCV) infection constitutes the leading indication for orthotopic LT (OLT) in the U.S., Europe and Japan. Unfortunately, reinfection of the graft represents a universal phenomenon after LT. The majority of patients with virological recurrence will develop histological graft injury, with about one-third of patients developing cirrhosis at only 5 years of follow-up (1–5). In addition, time interval from HCV cirrhosis to decompensation is significantly shorter in OLT recipients than in nontransplant patients (1–5). Not surprisingly, HCV is associated with decreased patient and graft survival when compared with other indications of OLT (1,5).

Factors associated with accelerated HCV recurrence (HCVrec) after LT include high viremia, donor age and quality (older than 55 years old), prolonged cold ischemia time, cytomegalovirus and immunosuppressant protocols.

Acute cellular rejection (ACR) after LT is common and remains an important cause of morbidity and late graft failure in the liver transplant recipient (LTR). Recent data suggest a variable rate of ACR between 18% and 30% (6). This tendency may be explained by the introduction of new and more potent immunosuppressant drugs in the last decade, capable of reducing the risk of ACR (6,7).

ACR rate after LT is especially controversial in HCV-positive recipients because of the overlapping of clinical and histological features with HCVrec. Reports suggest that the incidence of ACR may be in the range of 40% to 49% in HCV-positive recipients 6 months after LT (7). The high discrepancy of ACR incidence in HCV patients is explained by

the difficulty on the differential diagnoses, which represents one of the most critical challenges in the liver transplant community. Furthermore, accurate diagnosis remains a critical issue, since associated therapy may lead to worse graft and patient survival (6–10). It is well documented that pulse intravenous corticosteroid bolus treatment for ACR exacerbates HCV infection, inducing transient 1- to 2-log increased HCV RNA levels and thus increasing mortality and graft loss (5,7,11,12).

There is a critical need for biomarkers capable of accurately differentiating between these two entities after LT. Despite some promising results, discovery of reliable diagnostic biomarkers is still lacking. Whole genome oligonucleotide microarrays represent a powerful technology to study thousands of genes simultaneously and concomitantly to discover new biomarkers for diagnosis, prognosis and treatment of complex and multifactorial diseases. In the present report, we evaluate differential gene expression, using microarrays in liver samples from HCV transplant recipients with HCVrec disease, and ACR in the setting of HCV infection.

MATERIALS AND METHODS

Patients and Tissue Samples

The Institutional Review Board approved the study at Virginia Commonwealth University. Written informed consent was obtained from all patients. A total of 53 liver samples from unique HCV LT recipients were used for this study. As the training set, 32 fresh-frozen liver tissue samples were obtained for clinical indication: 22 tissues from patients with HCVrec and 10 with ACR in the setting of HCV infection (all diagnosed by histopathological examination). In addition, two fresh-frozen tissue samples from HCV seronegative post-LT recipients and with histological diagnosis of ACR were included. Furthermore, an independent set of 19 biopsy samples histologically diagnosed with HCVrec (n = 9) and HCV-ACR (n = 10) were eval-

uated as the validation set. Demographic and clinical characteristics of both training and validation sets of patients were collected.

RNA Isolation, cDNA Synthesis and *In Vitro* Transcription for the Labeled cRNA Probe

Tissue samples were snap-frozen in liquid nitrogen or collected in RNA Later solution (Ambion, Austin, TX, USA) and stored at –80°C until use. Total RNA was extracted using TRIzol (Life Technologies, Carlsbad, CA, USA) by strictly following the Affymetrix GeneChip® Expression Analysis Manual (Affymetrix, Santa Clara, CA, USA). Total isolated RNA sample preparation follows purity and integrity quality control parameter criteria previously established in our laboratory (13). cDNA synthesis, *in vitro* transcription for labeled cRNA probe, Affymetrix HGU133A version 2.0 GeneChip® hybridization, as well as array image generation and probe sets reading and expression analysis were performed as described previously (13).

Data Analysis

To identify probe sets significantly differentially expressed from hybridized microarrays and among the three samples groups, probe set level analysis of variance models were fit considering probe set expression as the response and tissue type (HCVrec, HCV-ACR and no-HCV-ACR) as the fixed effect of interest. A group's mean parameterization of tissue type was included as the fixed effect term to facilitate extraction of linear contrasts of interest. To adjust data for multiple comparisons, probe sets with P values from the overall F test <0.005 were considered significant. Thereafter, among probe sets identified as differentially expressed via the F test, all pair-wise comparisons were performed. The *limma* package was used to fit the mixed-effects models using restricted maximum likelihood procedure. Also, an empirical Bayes method was applied to moderate probe set standard

errors by borrowing information across the entire group.

Statistical Predictive Class Analysis

The last absolute shrinkage and selection operator (LASSO) L1-penalized method was performed as a classifier for HCVrec versus HCV-ACR as a predicted dependent variable. The relevance and effectiveness of penalized methods, more specifically for LASSO, when modeling microarray data to identify important genes, was previously described (14). The LASSO model was fit using the *glmpath* package (15) in the R programming environment (16) using an appropriate Bioconductor package (17). All probe sets identified as significantly differentially expressed when comparing HCVrec (n = 22) to HCV-ACR (n = 10) were included into the analysis. N-fold cross-validation was performed to provide an unbiased estimate of generalization error when classifying groups and thus to validate the accuracy and analytical performance of the best-fitted model.

Interaction Network and Functional Analysis

Gene ontology and interaction were analyzed with the Ingenuity Pathways Analysis (IPA) tool 8.7 (http://www. ingenuity.com). Lists of specific genes were generated from each corresponding supervised analysis obtained for each pair-wise comparison. Also, the IPA tool was used to analyze the biological role of those genes identified by the best-fitting LASSO model. All gene lists generated from pair-wise comparisons and containing probe set IDs, Entrez gene IDs as clone identifiers and fold-change values were mapped in the Ingenuity Knowledge Base (genes + endogenous chemicals) as the reference set. A similar analysis was performed for those differentially expressed probe sets representing genes identified as specifics for HCVrec versus HCV-ACR (Table 1). Biological role and disease relevance were established for each specific gene list through the associated

Table 1. Exclusive genes differentially expressed between HCVrec and HCV-ACR.

Affymetrix ID	Gene symbol	Entrez gene name	P
206506_s_at	SUPT3H (includes EG:8464)	Suppressor of Ty 3 homolog (S. cerevisiae)	0.0019
214473_x_at	PMS2L3	Postmeiotic segregation increased 2-like 3	0.0008
211558_s_at	DHPS	Deoxyhypusine synthase	0.0009
202120_x_at	AP2S1ᵃ	Adaptor-related protein complex 2, sigma 1 subunit	0.0002
201765_s_at	HEXA	hexosaminidase A (α polypeptide)	0.0003
216032_s_at	ERGIC3	ERGIC and golgi 3	0.0005
216903_s_at	CBARA1	Calcium binding atopy-related autoantigen 1	0.0027
204985_s_at	TRAPPC6A	Trafficking protein particle complex 6A	0.0002
204601_at	N4BP1	NEDD4 binding protein 1	0.0003
201600_at	PHB2	Prohibitin 2	0.0002
212782_x_at	POLR2J	Polymerase (RNA) II (DNA directed) polypeptide J, 13.3 kDa	0.0016
202387_at	BAG1	BCL2-associated athanogene	0.0003
214277_at	COX11	COX11 cytochrome c oxidase assembly homolog (yeast)	0.0004
218679_s_at	VPS28	Vacuolar protein sorting 28 homolog (S. cerevisiae)	0.0004
220089_at	L2HGDH	L-2-hydroxyglutarate dehydrogenase	0.0001
218345_at	TMEM176A	Transmembrane protein 176A	0.0001
210927_x_at	JTB	Jumping translocation breakpoint	0.0003
213550_s_at	NDUFA2	NADH dehydrogenase (ubiquinone) 1 α subcomplex, 2, 8 kDa	0.0002
220532_s_at	TMEM176B	Transmembrane protein 176B	<0.0001
203927_at	NFKBIE	Nuclear factor of kappa light polypeptide gene enhancer in B-cells inhibitor, epsilon	0.0002
201119_s_at	COX8A	Cytochrome c oxidase subunit VIIIA (ubiquitous)	0.0003
221488_s_at	CUTA	cutA divalent cation tolerance homolog (E. coli)	0.0002
213540_at	HSD17B8	Hydroxysteroid (17-beta) dehydrogenase 8	0.0003
202283_at	SERPINF1	Serpin peptidase inhibitor, clade F (α-2 antiplasmin, pigment epithelium derived factor), member 1	0.0002
215084_s_at	LRRC42	Leucine rich repeat containing 42	0.0003
203024_s_at	C5ORF15	Chromosome 5 open reading frame 15	0.0002
219345_at	BOLA1	bolA homolog 1 (E. coli)	0.0005
209208_at	MPDU1	Mannose-P-dolichol utilization defect 1	0.0003
207157_s_at	GNG5	Guanine nucleotide binding protein (G protein), γ 5	0.0001
1861_at	BAD	BCL2-associated agonist of cell death	0.0003
48825_at	ING4	Inhibitor of growth family, member 4	0.0004
203478_at	NDUFC1	NADH dehydrogenase (ubiquinone) 1, subcomplex unknown, 1, 6 kDa	0.0001
218309_at	CAMK2N1	Calcium/calmodulin-dependent protein kinase II inhibitor 1	0.0001
208074_s_at	AP2S1ᵃ	Adaptor-related protein complex 2, sigma 1 subunit	0.0001
203857_s_at	PDIA5	Protein disulfide isomerase family A, member 5	0.0003
201023_at	TAF7	TAF7 RNA polymerase II, TATA box binding protein (TBP)-associated factor, 55 kDa	0.0005
201812_s_at	TOMM7	Translocase of outer mitochondrial membrane 7 homolog (yeast)	0.0006
203781_at	MRPL33	Mitochondrial ribosomal protein L33	0.0002
201560_at	CLIC4	Chloride intracellular channel 4	0.0014
211732_x_at	HNMT	Histamine N-methyltransferase	0.0022
204559_s_at	LSM7	LSM7 homolog, U6 small nuclear RNA associated (S. cerevisiae)	0.0005
204880_at	MGMT	O-6-methylguanine-DNA methyltransferase	<0.0001
204034_at	ETHE1	Ethylmalonic encephalopathy 1	<0.0001
220016_at	AHNAK	AHNAK nucleoprotein	0.0001
205750_at	BPHL	Biphenyl hydrolase-like (serine hydrolase)	0.0004
220942_x_at	FAM162A	Family with sequence similarity 162, member A	0.0001
219479_at	KDELC1	KDEL (Lys-Asp-Glu-Leu) containing 1	0.0003
201028_s_at	CD99 (includes, for example, 4267)	CD99 molecule	0.0001
217963_s_at	NGFRAP1	Nerve growth factor receptor (TNFRSF16) associated protein 1	0.0003
217289_s_at	SLC37A4	Solute carrier family 37 (glucose-6-phosphate transporter), member 4	0.0003

Continued

Table 1. *Continued.*

206262_at	ADH1C (includes, for example, 126)	Alcohol dehydrogenase 1C (class I), γ polypeptide	0.0025
212282_at	TMEM97	Transmembrane protein 97	0.0002
218459_at	TOR3A	Torsin family 3, member A	0.0001
202427_s_at	BRP44	Brain protein 44	0.0003
207621_s_at	PEMT	Phosphatidylethanolamine N-methyltransferase	0.0001
201316_at	PSMA2	Proteasome (prosome, macropain) subunit, α type, 2	0.0005
204284_at	PPP1R3C	Protein phosphatase 1, regulatory (inhibitor) subunit 3C	0.0001
220445_s_at	CSAG2	CSAG family, member 2	0.0003
207097_s_at	SLC17A2	Solute carrier family 17 (sodium phosphate), member 2	0.0001
210797_s_at	OASL	2′-5′-Oligoadenylate synthetase-like	0.0004
203946_s_at	ARG2[a]	Arginase type II	<0.0001
219230_at	TMEM100	Transmembrane protein 100	0.0001
205968_at	KCNS3	Potassium voltage-gated channel, delayed-rectifier, subfamily S, member 3	0.0006
208241_at	NRG1	Neuregulin 1	0.0007
211743_s_at	PRG2	Proteoglycan 2, bone marrow (natural killer cell activator, eosinophil granule major basic protein)	0.0001
204076_at	ENTPD4	Ectonucleoside triphosphate diphosphohydrolase 4	0.0002
203168_at	ATF6B	Activating transcription factor 6 beta	<0.0001
202106_at	GOLGA3	Golgin A3	0.0005
219944_at	CLIP4	CAP-GLY domain containing linker protein family, member 4	0.0003
37986_at	EPOR	Erythropoietin receptor	0.0004
218792_s_at	BSPRY	B-box and SPRY domain containing	0.0002
203945_at	ARG2[a]	Arginase type II	0.0001
221854_at	PKP1	Plakophilin 1 (ectodermal dysplasia/skin fragility syndrome)	0.0007

Pair-wise comparison was performed as HCVrec versus HCV-ACR. Significant differential gene expression is indicated by *P* values for each molecule.
[a]*ARG2* gene is represented by two different probe sets.

network functions and canonical pathways analysis.

Reverse Transcription and Real-Time PCR (RT-qPCR) for an Independent Validation Set of Samples

Reverse transcription reactions were performed using TaqMan® Reverse Transcription Reagents (Applied Biosystems, Foster City, CA, USA) and according to the manufacturer protocol. Real-time PCRs (qPCRs) were carried out in an ABI Prism 7700 Sequence Detection System, using TaqMan® Gene Expression Assays (Applied Biosystems) (*ARG2*: Hs00982833_m1, *ETHE1*: Hs00204752_m1, *TMEM176A*: Hs00218506_m1 and *TMEM176B*: Hs00962650_m1). Gene expression fold-changes were obtained using the ΔCt calculation model between the target gene mean cycle threshold (Ct) and β2-microglobulin (B2M) Ct as endogenous control, or ΔCt (gene) – ΔCt (B2M). A two-tailed *t* test was performed to compare the mean expression between HCVrec and HCV-ACR samples for all validated genes. A *P* value <0.05 was considered significant.

All supplementary materials are available online at www.molmed.org.

RESULTS

Patients

Clinicopathological characteristics of the 51 LT patients are fully described in Supplementary Table S1 (A,B). All patients (except the two no-HCV patients with ACR) included into this study were diagnosed with HCV infection, genotype 1b before LT, and were the primary transplant, and all patients received an HCV-negative graft from a standard deceased donor. The immunosuppression protocol was similar for all patients and consisted of calcineurin inhibitor (tacrolimus, cyclosporine)-based therapy and steroid induction. The steroid-based therapy was routinely discontinued 3 months after LT in all cases.

Genomic Clustering of Liver Biopsy Samples

A total of 22,098 probe sets (>91%) were identified as present in each hybridized microarray generated for each tissue sample diagnosed with HCVrec (n = 32) and HCV-ACR and no-HCV-ACR (n = 19). Afterward, control probe sets were removed and the gene expression data set was further restricted to include only those probe sets declared to be either present or marginally present in at least 50% of the samples with an expression standard deviation among the 99th percentile or higher. Unsupervised hierarchical clustering analysis was performed to determine the natural sample clustering (Figure 1). The generated heatmap and dendrogram grouped most of HCVrec samples (68%; 15/22) in a defined cluster. A similar trend was observed for the majority of HCV-ACR samples. In addition, one HCV-ACR sample was found to be clustered independently from both main groups. The
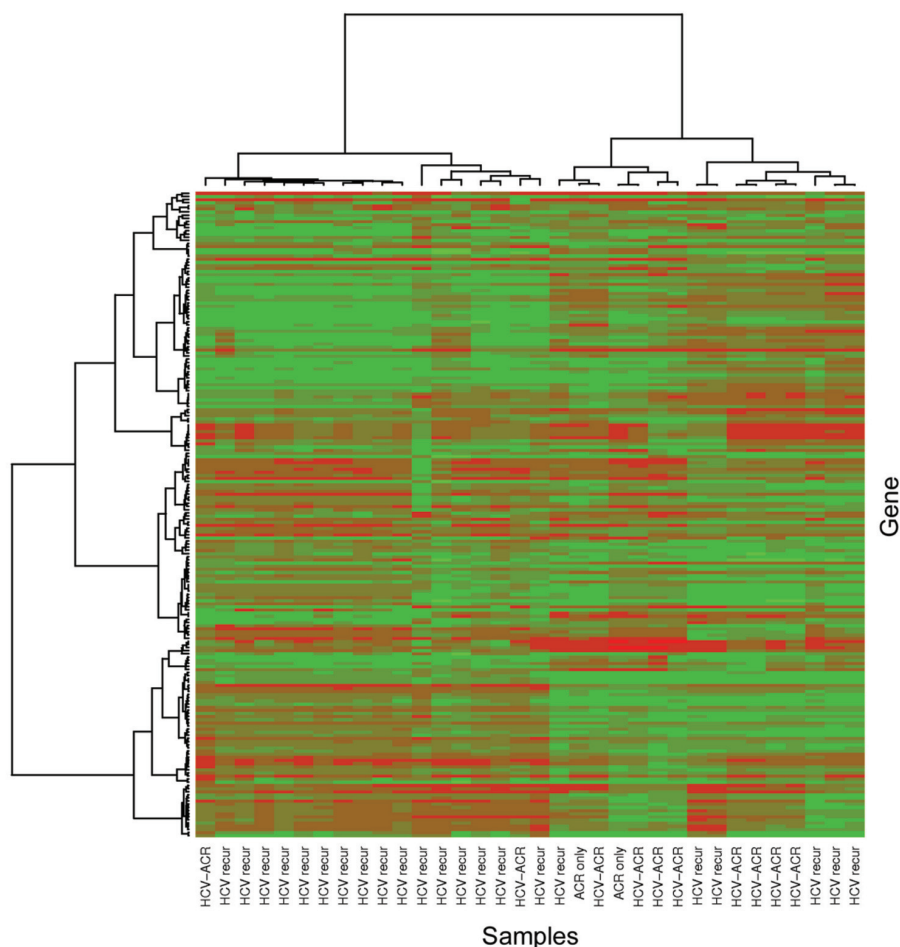
Figure 1. Unsupervised hierarchical clustering that includes all samples from the training group. Heatmap and dendrogram were generated using Ward's method with 1 – |Pearson correlation| as the distance measure, including probe sets declared to be either present or marginally present in at least 50% of samples and having an expression standard deviation among ≥99th percentile. HCV recur, HCV recurrence; ACR only, no-HCV-ACR.

misclassified profile may be a result of intrinsic clinicopathological features particular for each patient. Nevertheless, this analysis further suggested the possibility to differentiate both pathological conditions through the study of the differential genomic profile.

Identification of Differentially Expressed Probe Sets Among Sample Clusters

To better define a differential genomic profile within conditions, only probe sets exhibiting P values ≤0.001 were considered significant. A total of 179 probe sets were identified as significantly differentially expressed among three diagnostic

groups (HCVrec, HCV-ACR and no-HCV-ACR). All multiple pair-wise comparisons were performed to better define the relevance of those significant probe sets (Figure 2A). From this analysis, 123 (116 genes), 98 (94 genes) and 12 (12 genes) probe sets were found to be significantly differentially expressed among HCVrec versus HCV-ACR, and HCVrec versus no-HCV-ACR, and HCV-ACR versus no-HCV-ACR, respectively. From the analysis of each pair-wise comparison, 80 probe sets (71 genes) were identified as exclusively differentially expressed between HCVrec and HCV-ACR. When the analysis was performed for HCVrec versus no-HCV-ACR, 47 probe

sets (36 genes) were identified as significant (Figure 2A). Furthermore, only one probe set was exclusively identified between ACR tissue samples regarding the HCV infection state of the patient. Those ACR tissue samples were incorporated to identify genes specifically associated with this post-LT complication independent of HCV setting. Thus, this finding suggests independent characteristics for ACR, regardless of the recipient's clinical feature.

Supervised Genomic Clustering

Those specific probe sets identified by pair-wise comparison between HCVrec and HCV-ACR were analyzed to identify a characteristic molecular signature. From the analysis of those 71 genes specifically differentially expressed between groups, 59 genes (83%) were preferentially expressed in HCVrec samples, whereas the remaining 17% (12 genes) were identified in ACR-HCV (Table 1). The probe set intensity values representing those exclusive genes were used to conduct a supervised hierarchical clustering analysis (Figure 2B). The generated heatmap and dendrogram identified most HCVrec and HCV-ACR samples tightly clustered in two independent groups. Importantly, those no-HCV-ACR samples clustered within the HCV-ACR group in favor of the negligible differential gene expression between both ACR origins.

Biological Function Analysis of HCVrec and HCV-ACR Exclusive Genes

Core analysis was performed to interpret the data set in the context of biological processes, pathways and molecular networks those specific genes differentially expressed when comparing HCVrec with HCV-ACR. HCVrec-related genes were found to be preferentially associated with cell death regulation (P = 9.55E-04–4.55E-02), cell morphology (P = 1.59E-03–4.55E-02), carbohydrate (P = 3.32E-03–4.23E-02), amino acid metabolism (P = 3.32E-03–2.30E-02) and cellular development (P = 3.32E-03–2.30E-02). From the analysis of HCV-
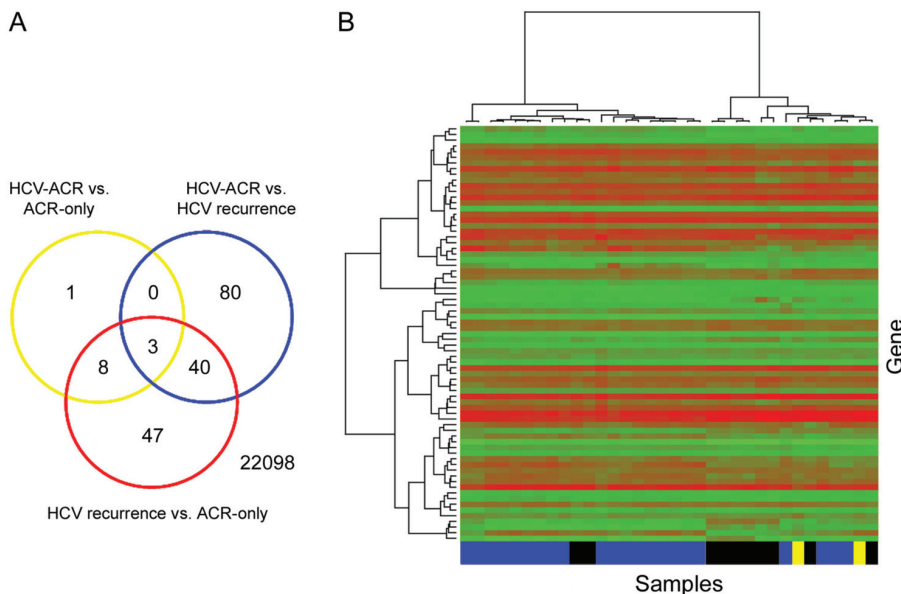
A

B

Figure 2. (A) Venn diagram illustrating the number of significant probe sets for the three pair-wise comparisons. 22098: total analyzed probe sets. (B) Supervised hierarchical clustering restricted to the 80 exclusive probe sets (71 genes) significantly differentially expressed between HCVrec and HCV-ACR samples (see Table 1). Heatmap and dendrogram were generated using Ward's method with 1 – |Pearson correlation| as the distance measure. Blue boxes, HCV recurrence; black boxes, HCV-ACR; yellow boxes, no-HCV-ACR (ACR-only).

ACR–related genes, the identified canonical pathways were significantly implicated in cell growth and proliferation ($P = 7.11E-04–4.93E-02$), cell cycle ($P = 7.76E-04–1.47E-02$), cell-to-cell signaling and interaction ($P = 7.76E-04–4.88E-02$) and cellular assembly and organization ($P = 7.76E-04–3.06E-02$) (Supplementary Table S2). The overview of this analysis clearly suggests different cellular mechanisms involved in both post-LT pathological conditions.

Association of the Differentially Expressed Genes with Pathological Conditions

To better differentiate both conditions, the role and impact of these differentially expressed genes in disease development were analyzed using the IPA tool (www.ingenuity.com).

From the analysis, 32% (19/59) of HCVrec-deregulated genes were significantly associated with disease molecular pathways involved in cancer development (17 molecules; $P = 1.42E-03$ to

4.60E-02) and gastrointestinal disease (6 molecules; $P = 6.42E-03$ to $3.27E-02$). A group of cancer-associated genes was found to be involved in T cytotoxic lymphocyte development (*adaptor-related protein complex 2, sigma 1 subunit* [*AP2S1*]) and adhesion to endothelium (*CD99*), T-cell lymphoma (*serpin peptidase inhibitor, clade F [α-2 antiplasmin, pigment epithelium derived factor], member 1* [*SERPINF1*], and *O-6-methylguanine-DNA methyltransferase* [*MGMT*]), pro-apoptotic genes related to B and T lymphocytes regulation (*BCL2-associated agonist of cell death* [*BAD*]) and apoptosis of activated T cells (*nuclear factor of kappa light polypeptide gene enhancer in B-cells inhibitor, epsilon* [*NFKBIE*]). The analysis result also identified other pro-apoptotic genes (*inhibitor of growth family, member 4* [*ING4*]), transforming growth factor (TGF)-β–regulated genes involved in Histamine metabolism (*histamine N-methyltransferase* [*HNMT*]), nitric oxide and reactive oxygen species production in macrophages (*protein phosphatase 1, regulatory [inhibitor] subunit 3C* [*PPP1R3C*])

and immune modulation–related genes through proteasome degradation of the major histocompatibility complex (MHC) class I molecule (*proteasome [prosome, macropain] subunit, α type* [*PSMA2*]). *HNMT* and *hexosaminidase A* (*HEXA*) genes were found to be associated with rheumatoid arthritis, an inflammatory disease with high predominance of activated T cells. Moreover, the *2′-5′-oligoadenylate synthetase-like* (*OASL*) encoding gene, positively related to high HCV load (18), was also differentially expressed in HCVrec disease patients.

Analysis of the HCV-ACR genomic pattern revealed most of the deregulated genes are further associated with inflammatory response and disease, such as airway hypersensitive reaction through induction of eosinophil, basophil and neutrophil degranulation (*proteoglycan 2* [*PRG2*]) and nitric oxide degradation (*ARG2*). The *neuregulin-1 encoding gene* (*NRG1*) was also found to be associated with the development of hypersensitive reactions. Additionally, other genes were found to be involved in the development of atopic dermatitis (*ectonucleoside triphosphate diphosphohydrolase 4* [*ENTPD4*]) and rheumatoid arthritis (*potassium voltage-gated channel, delayed-rectifier, subfamily S, member 3* [*KCNS3*]; *erythropoietin receptor* [*EPOR*]; and *activating transcription factor 6 beta* [*ATF6B*]).

Overall, these results propose that a cytotoxic component may be exerted by a tuned T-cell-mediated cytolysis in response to virus-infected cells in HCVrec samples. The role of HCV-ACR–related genes suggests allograft damage may be caused by an adaptive immune response as an immediate hypersensitivity reaction and also may be through a T-cell immunoreaction trend.

Predictive Model that Uses the L1 Penalized Method

The LASSO (L1)-penalized method was performed as a classifier for HCVrec versus HCV-ACR to identify most important genes. The best-fitting LASSO model was subsequently confirmed using the *N*-fold cross-validation method

Table 2. Genes identified by the best-fitting LASSO model.

Affymetrix ID	Entrez ID	Gene symbol	Coefficient estimate[a]
212619_at	23306	TMEM194A	–5.33
207367_at	479	ATP12A	–4.56
212056_at	23199	KIAA0182	–3.89
213515_x_at	3048	HBG2	–1.16
203946_s_at	384	ARG2[a]	–1.12
212856_at	23151	GRAMD4	–0.82
212993_at	138151	BTBD14A	–0.55
206214_at	7941	PLA2G7	–0.44
201502_s_at	4792	NFKBIA	0.19
206293_at	6822	SULT2A1	0.26
204034_at	23474	ETHE1[a]	0.39
205251_at	8864	PER2	0.52
202732_at	11142	PKIG	0.61
220532_s_at	28959	TMEM176B[a]	1.36
218345_at	55365	TMEM176A[a]	2.00

[a]Coefficients estimated by the LASSO model reflect the log odds of having HCV-ACR.
[b]Genes identified as exclusive by the LASSO model and HCVrec versus HCV-ACR pair-wise comparison (see also Table 1).

as described in previous reports from our laboratory (14). The genomic pattern displayed by the best-fitting LASSO model included 15 probe sets differentially expressed for HCV-ACR (eight genes) and HCVrec disease (seven genes), listed in Table 2. Except *nuclear factor of kappa light polypeptide gene enhancer in B-cells inhibitor, alpha* (*NFKBIA*), all genes were also present in the differentially expressed probe sets identified by pairwise comparisons. More importantly, the *N*-fold cross-validation estimated error rate for the best-fitting model was 21.9%, which indicates a classifier accuracy rate of 78.1%. The classifier rates for sensitivity, specificity and positive and negative predictive values were 50.0%, 90.9%, 71.4% and 80.0%, respectively. Interestingly, 4 of those 15 genes (1 associated with HCV-ACR [*ARG2*] and 3 associated with HCVrec [*ETHE1*, *TMEM176A* and *TMEM176B*]) were also included into the characteristic molecular signature identified between HCVrec and HCV-ACR (Tables 1 and 2).

Biological function analysis associated those genes with cell death, gene expression and cell cycle progression as top scored network functions (score >26), along with molecular transport, lipid metabolism, cellular movement and protein

synthesis pathways. HCVrec differentially expressed genes were found to be associated with IFN-γ positive gene expression regulation (*period homolog 2 (Drosophila)* [*PER2*] [19]); NFKB signaling pathway involved in regulation of T-cell proliferation, activation and apoptosis (*NFKBIA* and *ETHE1* [20,21]); dehydroepiandrosterone sulfation and detoxification of bile acids (*SULT2A1*), which was downregulated in the lipopolysaccharide (LPS)-induced acute-phase response (22); cAMP-dependent protein kinase (PKA) signaling inhibitor (*PKIG* [23]); and genes involved in the maintenance of the immature state of dendritic cells (*TMEM176A* and *TMEM176B* [24]) (Table 2). In a different trend, HCV-ACR–associated genes were found to be preferentially involved in the proinflammatory process related to hypersensitive reaction and apoptosis regulation (*phospholipase A2, group VII (platelet-activating factor acetylhydrolase, plasma)* [*PLA2G7*]; *ARG2*; *GRAM domain containing 4* [*GRAMD4*]), oxygen transport activity and severe acute respiratory syndrome (*hemoglobin, gamma G* [*HBG2*]). Of note, the arginase 2 encoding gene (*ARG2*) exerts an anti-apoptotic role through the negative modulation of nitric oxide (25), and its expression was found to be in-

creased during eosinophil inflammatory reaction in asthma via the Th2 lymphocyte profile induced by interleukin (IL)-4 and IL-13 (26,27). The platelet-activating factor–acetylhydrolase enzyme encoding gene (*PLA2G7*) is a proinflammatory factor associated with atherogenic plaque formation (28,29) and apoptosis inhibition through oxidized phospholipid hydrolization (30). The cellular function of GRAMD4 was postulated as similar to the p53 apoptosis regulatory factor (31). ATP12A is related with ATPase H(+) and K(+) ions exchange, and no specific cellular role has yet been established for *TMEM194A*, *KIAA0182* and *BTBD14A* (Table 2).

To sum up, the HCVrec-associated genes identified by the LASSO predictive model are preferentially involved in an innate immune response, whereas HCV-ACR–related genes suggest a strong proinflammatory and antiapoptotic activity more related to an adaptive immune response that may be associated to a Th2 context

Gene Expression Validation in an Independent Set of Samples

A set of genes was selected for further evaluation in an independent set of samples using the following criteria: (a) differentially expressed genes between HCVrec and HCV-ACR and (b) identification in the best LASSO model. The expression levels of *ARG2*, *ETHE1*, *TMEM176A* and *TMEM176B* genes, all identified by supervised analysis and the LASSO model, were validated in an independent sample set by qPCR. From the analysis, all genes were found to be significantly and differ-

Table 3. Gene expression validation in an independent set of samples.

Gene ID	qPCR fold-change	P
ARG2	2.1 ± 1.3	0.032
ETHE1	4.2 ± 0.8	0.010
TMEM176A	2.0 ± 0.9	0.034
TMEM176B	2.1 ± 0.8	0.017

Additional data regarding each gene are detailed in Tables 1 and 2.

entially expressed between both post-LT conditions. More importantly, there was a perfect correlation between both expression profiles identified by microarrays (training set) and RT-qPCR (validation set), as shown in Table 3.

DISCUSSION

Liver biopsy is currently considered the gold standard for the histopathological evaluation of complications occurring on the graft after LT. However, differentiation of HCVrec from ACR in HCV LT recipients is especially challenging and provides conflicting results, even among experienced liver pathologists (32–37).

Importantly, therapy selection and efficacy further relies on the accuracy of the diagnosis. Actually, an ambiguous or uncertain diagnosis may induce a detrimental manner on the graft and patient survival rates (7,11).

In the recent years, a substantial number of markers were postulated as potential biomarkers of disease differentiation. Recent studies on immunohistochemistry assays proposed the end product of activated complement cascade component C4 (C4d) as a promising biomarker to differentially diagnose HCVrec from ACR (36,37). Unfortunately, these findings were not able to be validated by a prospective study using an enzyme-linked immunosorbent assay–based test (38). In addition, MxA and IFI16 interferon-inducible proteins (39,40) and the lymphocyte-expressed Mcm-2 protein (35) were also postulated as potential biomarkers, but prospective studies for further validation are lacking. The potential utility of the ImmunKnow assay for the post-LT immune function status of HCV recipients using biopsy samples was suggested by Cabrera *et al.* (41). Moreover, the findings from this report were further supported by Rubinas *et al.* (42) and others (43). However, the reliable availability and accuracy of biomarkers to support or replace histopathology is scarce.

Microarray technology represents an excellent tool to elucidate differential gene expression patterns and establish accurate molecular markers for differential disease diagnosis (44). There are two previous reports that aimed to differentiate ACR and HCVrec by genomic studies (45,46). These reports showed gene expression profiles characterizing the two subgroups of HCV patients. However, in the study performed by Sreekumar *et al.* (46), the signatures were not validated in an independent set of patients. Also, both reports lack inclusion of ACR samples from recipients with no HCV infection.

In the present study, we successfully performed whole genome analysis using GeneChip microarrays to differentiate biopsy-proven HCVrec disease from ACR in the setting of HCV infection. From this study, we identified a gene signature composed of 71 molecules differentially expressed between HCVrec (59 genes) and ACR (12 genes). The biological analysis of the cellular function of those genes associated with HCVrec revealed a strong hepatocyte cytotoxicity component represented by genes involved in regulation of proliferation, growth, adhesion and apoptosis of cytotoxic T lymphocytes and regulated by canonical pathways such as IFN-γ and nuclear factor κB. In comparison, the biological role of genes identified as exclusive for ACR in the setting of HCV infection suggested an association of the allograft damage through an immediate hypersensitivity reaction. This result may be triggered by eosinophil and neutrophil cell degranulation (major basic protein-1 encoding gene [*PRG2*]), along with the possibility of atherosclerosis development, mainly due to the presence of macrophage-related metabolic genes. It is interesting to note that some genes exclusively identified in ACR were associated with atherosclerosis development (such as *PLA2G7* [28,29]) and nitric oxide degradation (such as *ARG2* [25]), which may be involved in the hepatic vein endothelium injury mechanism characteristic of this post-LT complication.

Sreekumar *et al.* (46) previously reported a differential gene expressed between well-characterized HCVrec and ACR, but this report suggested that the HCVrec pathological component is more related to HCV infection cytopathic effects rather than the immune-mediated process. Also, the authors related the differential expression of IL-2, IFN-γ and tumor necrosis factor (TNF)-α encoding genes to ACR, whereas other authors found increased IL-4 and IL-10 gene expression (47). Furthermore, other reports suggest that the pathophysiological mechanisms of both entities are mainly characterized by a T-lymphocyte infiltrate, and although the distinction is difficult when overlapping occurs, the fine immune cell functions tuning and localization indicate that those conditions are completely different (4,7). In a timeline, HCVrec mostly begins 3–8 weeks after LT, whereas ACR begins mostly within 60–90 days. However, it is well known that the time of occurrence of these two complications overlaps (4).

Histopathologically, HCVrec is characterized by lobular hepatitis featured by mottled apoptotic hepatocytes and inflammation generated by a Th-1 type lymphocytic immune reaction (INF-γ, TNF-α, IL-2 and IL-12) with predominant cytotoxic T cells (mostly CD8^{+}) aimed at directly eliminating infected hepatocytes. In combination, high HCV viral replication induces oxidative stress and ineffective antiviral immune response, contributing to the inflammatory scenario through activation of the Fas ligand apoptotic pathway and inducing hepatocyte lysis through the perforin/granzyme system (4,48,49). ACR is histologically characterized by inflammatory infiltrates of portal tracts, bile ducts and hepatic vein endothelium by CD4^{+} and CD8^{+} T lymphocytes and macrophages, as dominant cell types and together with eosinophil cells (4,6). Furthermore, in addition to T cells, B lymphocytes and plasma cells were also suggested to be present in ACR infiltrates (7,50). The identified gene expression profiles in the present study correlate with the predicted signatures for the cells described as involved in the

characteristic histological features for both HCVrec and HCV-ACR.

Little is known about the ACR condition in the presence and absence of a viral immune reaction scenario. We performed genomic comparative studies to further characterize differential gene expression between ACR alone and in the setting of HCV graft infection, but interestingly, no further significant differences were identified (Figure 2A). These results are of high interest because they strongly indicate that ACR immune reaction is independent of viral infection backgrounds, at least through gene expression modulation. Nevertheless, it was postulated that the generated inflammatory microenvironment by acute HCV reinfection in combination with partial donor-recipient MHC class I compatibility may trigger an ACR response by enabling MHC-restricted HCV-specific cytotoxic T cells to target alloantigens (4,7). In this sense, immune-modulatory–related genes by the MHC class I molecule proteasome degradation (*PSMA2*) and maintenance of the immature state of dendritic cells (*TMEM176A*, *TMEM176B*) were identified as specific for HCVrec. The immature state of dendritic cells was related to the silencing of antigen-specific T cells, thus avoiding an autoimmune reaction (51). Thus, an early imbalance of the expression of this kind of gene might contribute to the ACR triggering in the acute graft HCV infection.

To gain insight into the diagnostic impact of the generated genomic signature, supervised hierarchical clustering was performed, and all patients were classified into two major groups as HCVrec and HCV-ACR (Figure 2B). It is interesting to note that all cases of ACR from patients with no HCV infection were clustered within HCV-ACR samples. This clustering pattern is in agreement with the observed null differential genomic expression between both ACR origins and further corroborates the unique nature of this particular post-LT condition. Also, from the analysis, it is possible to distinguish six samples (two from HCV-ACR and four from HCVrec) as misclas-

sified. Interestingly, reinspection of the pathology report of those HCV-ACR samples revealed mixed histological features with more prominent pan-lobular inflammation and hepatocytes apoptosis and resolved ACR. In contrast, those misclassified HCVrec samples showed histological characteristics of extensive fibrosis and inflammation together with macrovesicular steatosis. In addition, the HCV serum load was found one log lower with respect to other patients, and two of them were directly negative. In conclusion, these cases represent why diagnosis is difficult and show the risk of misdiagnosing post-LT patients because of unclear histopathological reports. These findings further support the potential utility of molecular markers in the differential diagnosis.

Hereby, we proposed a set of genes capable of differentiating both conditions with high accuracy (LASSO), which was further validated in an independent group of well-diagnosed patients. Furthermore, it was possible to determine through the absence of major genomic differences that ACR is a HCV-independent immunological reaction post-LT. More importantly, we proposed a set of four validated genes as potential biomarkers for differential diagnosis of both complications: HCVrec and ACR. Altogether, our findings are of high importance for the accurate diagnosis of both entities, with a concomitant high impact on the selection of suitable therapy. Nevertheless, subsequent cohort studies must be performed and aimed to further validate the identified molecular markers.

ACKNOWLEDGMENTS

DISCLOSURE

The authors declare that they have no competing interests as defined by *Molecular Medicine*, or other interests that might be perceived to influence the results and discussion reported in this paper.

REFERENCES

1. Garcia-Retortillo M, *et al.* (2002) Hepatitis C virus kinetics during and immediately after liver transplantation. *Hepatology.* 35:680–7.
2. Gane EJ, *et al.* (1996) Long-term outcome of hepatitis C infection after liver transplantation. *N. Engl. J. Med.* 334:815–20.
3. Roche B, Samuel D. (2007) Risk factors for hepatitis C recurrence after liver transplantation. *J. Viral Hepat.* 14 Suppl 1:89–96.
4. Demetris AJ. (2009) Evolution of hepatitis C virus in liver allografts. *Liver Transpl.* 15 Suppl 2:S35–41.
5. Watt K, Veldt B, Charlton M. (2009) A practical guide to the management of HCV infection following liver transplantation. *Am. J. Transplant.* 9:1707–13.
6. Knechtle SJ, Kwun J. (2009) Unique aspects of rejection and tolerance in liver transplantation. *Semin. Liver Dis.* 29:91–101.
7. Burton JR Jr, Rosen HR. (2006) Acute rejection in HCV-infected liver transplant recipients: the great conundrum. *Liver Transpl.* 12:S38–47.
8. Kurian S, *et al.* (2007) Applying genomics to organ transplantation medicine in both discovery and validation of biomarkers. *Int. Immunopharmacol.* 7:1948–60.
9. Gelb B, Feng S. (2009) Management of the liver transplant patient. *Expert Rev. Gastroenterol. Hepatol.* 3:631–47.
10. Manousou P, *et al.* (2009) Outcome of recurrent hepatitis C virus after liver transplantation in a randomized trial of tacrolimus monotherapy versus triple therapy. *Liver Transpl.* 15:1783–91.
11. Demetris AJ, *et al.* (2004) Recurrent hepatitis C in liver allografts: prospective assessment of diagnostic accuracy, identification of pitfalls, and observations about pathogenesis. *Am. J. Surg. Pathol.* 28:658–69.
12. Berenguer M, *et al.* (2003) A model to predict severe HCV-related disease following liver transplantation. *Hepatology.* 38:34–41.
13. Mas VR, *et al.* (2006) Differentially expressed genes between early and advanced hepatocellular carcinoma (HCC) as a potential tool for selecting liver transplant recipients. *Mol. Med.* 12:97–104.
14. Archer KJ, *et al.* (2009) Identifying genes for establishing a multigenic test for hepatocellular carcinoma surveillance in hepatitis C virus-positive cirrhotic patients. *Cancer Epidemiol. Biomarkers Prev.* 18:2929–32.
15. Park MY, Hastie T. (2008) Penalized logistic regression for detecting gene interactions. *Biostatistics.* 9:30–50.
16. R Development Core Team. (2005) R: A Language and Environment for Statistical Computing [computer program]. Vienna (Austria): R Foundation for Statistical Computing. 2011 version available at: http://www.R-project.org.
17. Gentleman RC, *et al.* (2004) Bioconductor: open software development for computational biology and bioinformatics. *Genome Biol.* 5:R80.
18. Ishibashi M, Wakita T, Esumi M. (2010) 2′,5′-Oligoadenylate synthetase-like gene highly in-

duced by hepatitis C virus infection in human liver is inhibitory to viral replication in vitro. *Biochem. Biophys. Res. Commun.* 392:397–402.

19. Arjona A, Sarkar DK. (2006) The circadian gene mPer2 regulates the daily rhythm of IFN-gamma. *J. Interferon Cytokine Res.* 26:645–9.

20. Wang M, Windgassen D, Papoutsakis ET. (2008) A global transcriptional view of apoptosis in human T-cell activation. *BMC Med. Genomics.* 1:53.

21. Higashitsuji H, *et al.* (2002) A novel protein overexpressed in hepatoma accelerates export of NF-kappa B from the nucleus and inhibits p53-dependent apoptosis. *Cancer Cell.* 2:335–46.

22. Kim MS, Shigenaga J, Moser A, Grunfeld C, Feingold KR. (2004) Suppression of DHEA sulfotransferase (Sult2A1) during the acute-phase response. *Am. J. Physiol. Endocrinol. Metab.* 287:E731–8.

23. Chen X, Dai JC, Orellana SA, Greenfield EM. (2005) Endogenous protein kinase inhibitor gamma terminates immediate-early gene expression induced by cAMP-dependent protein kinase (PKA) signaling: termination depends on PKA inactivation rather than PKA export from the nucleus. *J. Biol. Chem.* 280:2700–7.

24. Condamine T, *et al.* (2010) Tmem176B and Tmem176A are associated with the immature state of dendritic cells. *J. Leukoc. Biol.* 88:507–15.

25. Mori M. (2007) Regulation of nitric oxide synthesis and apoptosis by arginase and arginine recycling. *J. Nutr.* 137:1616S–20S.

26. Kenyon NJ, Bratt JM, Linderholm AL, Last MS, Last JA. (2008) Arginases I and II in lungs of ovalbumin-sensitized mice exposed to ovalbumin: sources and consequences. *Toxicol. Appl. Pharmacol.* 230:269–75.

27. Zimmermann N, *et al.* (2003) Dissection of experimental asthma with DNA microarray analysis identifies arginase in asthma pathogenesis. *J. Clin. Invest.* 111:1863–74.

28. De Keyzer D, *et al.* (2009) Increased PAFAH and oxidized lipids are associated with inflammation and atherosclerosis in hypercholesterolemic pigs. *Arterioscler. Thromb. Vasc. Biol.* 29:2041–6.

29. Shi Y, *et al.* (2007) Role of lipoprotein-associated phospholipase A2 in leukocyte activation and inflammatory responses. *Atherosclerosis.* 191:54–62.

30. Chen R, Yang L, McIntyre TM. (2007) Cytotoxic phospholipid oxidation products: cell death from mitochondrial damage and the intrinsic caspase cascade. *J. Biol. Chem.* 282:24842–50.

31. John K, Alla V, Meier C, Putzer BM. (2010) GRAMD4 mimics p53 and mediates the apoptotic function of p73 at mitochondria. *Cell Death Differ.* 18:874–86.

32. Regev A, *et al.* (2004) Reliability of histopathologic assessment for the differentiation of recurrent hepatitis C from acute rejection after liver transplantation. *Liver Transpl.* 10:1233–9.

33. D'Errico-Grigioni A, *et al.* (2008) Tissue hepatitis C virus RNA quantification and protein expression help identify early hepatitis C virus recurrence after liver transplantation. *Liver Transpl.* 14:313–20.

34. Grassi A, *et al.* (2006) Detection of HCV antigens in liver graft: relevance to the management of recurrent post-liver transplant hepatitis C. *Liver Transpl.* 12:1673–81.

35. Unitt E, Gelson W, Davies SE, Coleman N, Alexander GJ. (2009) Minichromosome maintenance protein-2-positive portal tract lymphocytes distinguish acute cellular rejection from hepatitis C virus recurrence after liver transplantation. *Liver Transpl.* 15:306–12.

36. Jain A, *et al.* (2006) Characterization of CD4, CD8, CD56 positive lymphocytes and C4d deposits to distinguish acute cellular rejection from recurrent hepatitis C in post-liver transplant biopsies. *Clin. Transplant.* 20:624–33.

37. Schmeding M, *et al.* (2006) C4d in acute rejection after liver transplantation: a valuable tool in differential diagnosis to hepatitis C recurrence. *Am. J. Transplant.* 6:523–30.

38. Schmeding M, *et al.* (2010) ELISA-based detection of C4d after liver transplantation: a helpful tool for differential diagnosis between acute rejection and HCV-recurrence? *Transpl. Immunol.* 23:156–60.

39. MacQuillan GC, *et al.* (2010) Hepatocellular MxA protein expression supports the differentiation of recurrent hepatitis C disease from acute cellular rejection after liver transplantation. *Clin. Transplant.* 24:252–8.

40. Borgogna C, *et al.* (2009) Expression of the interferon-inducible proteins MxA and IFI16 in liver allografts. *Histopathology.* 54:837–46.

41. Cabrera R, *et al.* (2009) Using an immune functional assay to differentiate acute cellular rejection from recurrent hepatitis C in liver transplant patients. *Liver Transpl.* 15:216–22.

42. Rubinas T, Dellon E, Henel G. (2009) Use of an immune functional assay to differentiate recurrent hepatitis C from acute cellular rejection in liver transplant patients. *Liver Transpl.* 15:1157.

43. Hashimoto K, *et al.* (2010) Measurement of CD4+ T-cell function in predicting allograft rejection and recurrent hepatitis C after liver transplantation. *Clin. Transplant.* 24:701–8.

44. Maluf DG, Archer KJ, Villamil F, Stravitz RT, Mas V. (2010) Hepatitis C virus recurrence after liver transplantation: biomarkers of disease and fibrosis progression. *Expert Rev. Gastroenterol. Hepatol.* 4:445–58.

45. Asaoka T, *et al.* (2009) Differential transcriptome patterns for acute cellular rejection in recipients with recurrent hepatitis C after liver transplantation. *Liver Transpl.* 15:1738–49.

46. Sreekumar R, Rasmussen DL, Wiesner RH, Charlton MR. (2002) Differential allograft gene expression in acute cellular rejection and recurrence of hepatitis C after liver transplantation. *Liver Transpl.* 8:814–21.

47. Zekry A, *et al.* (2002) Intrahepatic cytokine profiles associated with posttransplantation hepatitis C virus-related liver injury. *Liver Transpl.* 8:292–301.

48. McCaughan GW, Shackel NA, Bertolino P, Bowen DG. (2009) Molecular and cellular aspects of hepatitis C virus reinfection after liver transplantation: how the early phase impacts on outcomes. *Transplantation.* 87:1105–11.

49. Ramirez S, Perez-Del-Pulgar S, Forns X. (2008) Virology and pathogenesis of hepatitis C virus recurrence. *Liver Transpl.* 14 Suppl 2:S27–35.

50. Krukemeyer MG, *et al.* (2004) Description of B lymphocytes and plasma cells, complement, and chemokines/receptors in acute liver allograft rejection. *Transplantation.* 78:65–70.

51. Ohnmacht C, *et al.* (2009) Constitutive ablation of dendritic cells breaks self-tolerance of CD4 T cells and results in spontaneous fatal autoimmunity. *J. Exp. Med.* 206:549–59.